Enhanced photothermal therapy assisted with gold nanorods using a radially polarized beam

Hong Kang, Baohua Jia, Jingliang Li, Dru Morrish, and Min Gu

Citation: Appl. Phys. Lett. **96**, 063702 (2010); doi: 10.1063/1.3302461
View online: http://dx.doi.org/10.1063/1.3302461
View Table of Contents: http://apl.aip.org/resource/1/APPLAB/v96/i6
Published by the American Institute of Physics.

Enhanced photothermal therapy assisted with gold nanorods using a radially polarized beam

Hong Kang, Baohua Jia, Jingliang Li, Dru Morrish, and Min Gu[a)]
Centre for Micro-Photonics, Faculty of Engineering and Industrial Sciences, Swinburne University of Technology, Hawthorn, Victoria 3122, Australia

(Received 20 November 2009; accepted 6 January 2010; published online 10 February 2010)

We report on the use of a radially polarized beam for photothermal therapy of cancer cells labeled with gold nanorods. Due to a three-dimensionally distributed electromagnetic field in the focal volume, the radially polarized beam is proven to be a highly efficient laser mode to excite gold nanorods randomly oriented in cancer cells. As a result, the energy fluence for effective cancer cell damage is reduced to one fifth of that required for a linearly polarized beam, which is only 9.3% of the medical safety level. © *2010 American Institute of Physics*. [doi:10.1063/1.3302461]

Nanoparticle-assisted photothermal therapy (PTT) of cancer cells has received much attention recently due to the fact that nanoparticles can be selectively attached to malignant cells. This opens the possibility for highly localized noninvasive therapy with minimized collateral damage to the surrounding healthy cells.[1–3] Among various types of nanoparticles, nontoxic gold nanorods (GNRs) have shown great potential owing to their strongly enhanced absorption and scattering induced by the coherent collective oscillation of electrons at their surface. Thus, simultaneous PTT and two-photon fluorescence (TPF) imaging of cancer cells can be realized in the focal volume.[4] Particularly, the size-dependent near infrared longitudinal absorption band of GNRs coincides the peak transmission window of skin and tissue (at wavelength 800 nm), making GNR assisted PTT and imaging more appealing in terms of a large penetration depth and a minimal destructive effect to healthy tissue.[4,5]

A linearly polarized laser mode has been extensively implemented in most experiments for GNR assisted PTT and imaging. Under such a circumstance, only a small portion of randomly oriented GNRs labeled to cancer cells can be effectively excited in the focal volume when their longitudinal axes are aligned with the excitation polarization direction.[6] This has led to a high threshold of laser energy fluence in biomedical applications. As a result, the irradiation power required to destruct the cancer cells is fatal to healthy tissue as well. Therefore, to make GNR assisted PTT and imaging a viable biomedical tool, it is necessary to explore proper laser modes to increase the excitation efficiency of GNRs and hence reduce the effective energy fluence to a level much lower than the medical safety level of 100 mJ/cm^2.[7]

In this letter we addressed this issue by introducing radially polarized beams to excite GNRs. Radially polarized beams are well known for their radial polarization orientation and distribution in free space. Once tightly focused by a high numerical aperture (NA) objective, a radially polarized beam results in a pronounced longitudinal polarization component in addition to the radially distributed transverse polarization component in the focal volume due to the depolarization effect.[8,9] It has been demonstrated that by using the radially polarized beams in GNR assisted PTT the energy fluence required to destruct the cancer cells is dramatically reduced to one fifth of that required for a linearly polarized beam.

In order to efficiently excite the randomly oriented GNRs, it is important to understand the polarization distribution of a laser beam in the focal volume. To this end, the vectorial-Debye diffraction theory[8] was employed to map the polarization distribution in the focal volume of a high NA (NA=1.2) objective at an excitation wavelength of 780 nm through a coverglass/water interface ($n_1/n_2=1.515/1.33$). For a linearly polarized beam along the x direction as shown in Figs. 1(a)–1(c), the dominant electromagnetic (EM) field component in the focal volume is parallel to the incident polarization direction with a peak ratio of the three polarization components in the x, y, and z directions, 1:0.0046:0.156. As a result, only the GNRs whose longitudinal axes are parallel with the x-z plane and not orthogonal to the EM field vector can be efficiently excited as illustrated in Fig. 1(d).

In comparison, under radial polarization illumination of the same power, as shown in Figs. 1(e)–1(h), a pronounced longitudinal component appears compared with the transverse component. The peak ratio of the three polarization components in the x, y, and z directions is 0.182:0.182:0.528. Through the redistribution of the transverse and the longitudinal components, the excitation of GNRs in all three dimensions can be possible [Fig. 1(h)]. The intensity at each point in the focal volume under radial polarization illumination is not necessarily larger than that under linear polarization illumination and the average intensity in the focal plane under radial polarization illumination is reduced by 30% compared with that under linear polarization illumination. Therefore, given the enhanced strength of the y and z polarization components in Figs. 1(e)–1(g), it is expected that a radially polarized beam can significantly enhance the PTT effects and the image contrast of randomly oriented GNRs compared with a linearly polarized beam.

In Fig. 2(a) the experimental setup for GNR assisted TPF imaging and PTT of cancer cells is presented. A linearly polarized ultrafast laser beam from a Ti:Sapphire laser with a repetition rate of 80 MHz and a pulse width of 80 fs at wavelength 780 nm (Spectra-Physics: Mai-Tai) was expanded to illuminate a radial polarization converter (RPC) (Arcoptix S.A.). The produced radially polarized beam was directed to a confocal optical microscopic system (Olympus:

[a)]Author to whom correspondence should be addressed. Electronic mail: mgu@swin.edu.au.

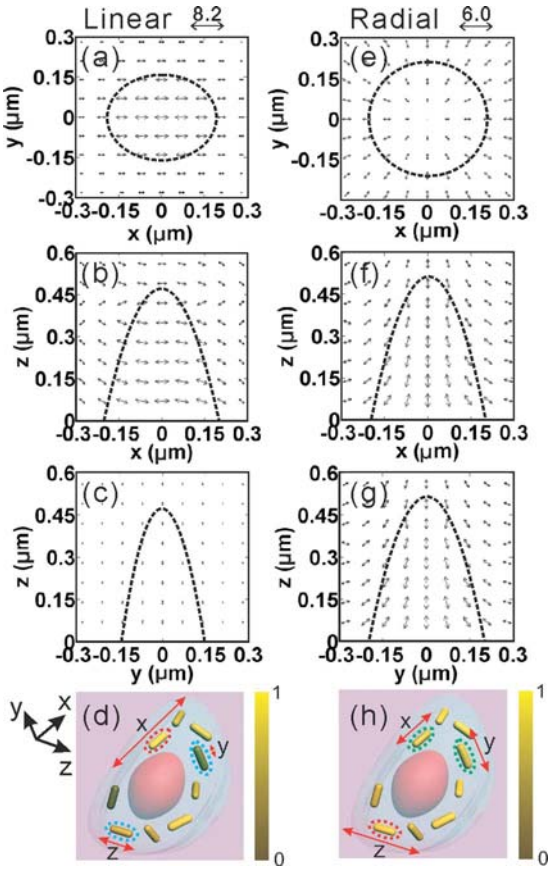

FIG. 1. (Color online) Polarization characteristics in the focal volume of a NA=1.2 objective under linear polarization (left) and radial polarization (right) illumination. [(a)–(c)] and [(e)–(g)] are the mapping of the EM field vectors projected on *x*-*y*, *x*-*z*, and *y*-*z* planes, respectively. (d) and (h) show the three-dimensional models for the excitation of GNRs in a cell. The arrows indicate the polarization directions and their length represents the strength of the EM field vector in the focal volume according to the scale bars on the top. Dashed curves represent the focal volume determined by the full width at half maximum. The color bars in (d) and (h) schematically denote the excitation strength of GNRs.

IX 70) with a water immersion objective (Olympus, NA =1.2). The incident power was controlled by a variable neutral density (ND) filter and measured in the focal spot. The mapping of the intensity distribution under radial polarization illumination using near-field optics has been reported

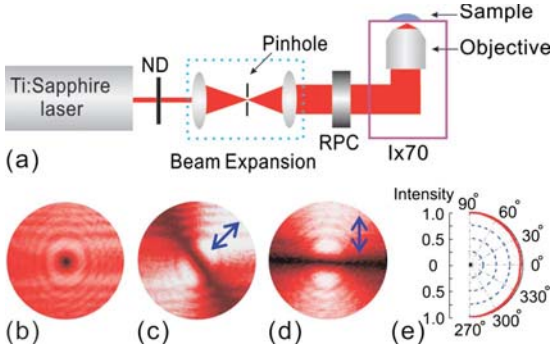

FIG. 2. (Color online) (a) Experimental setup for cancer imaging and therapy. ND: variable neutral density filter, RPC objective: NA=1.2, 60×, water immersion. (b) A typical hollow profile of a radially polarized beam in free space. (c) and (d): experimental intensity patterns when the analyzer is placed at 45° and 90° with respect to incident polarization, respectively. (e) Intensity distribution of the radially polarized beam at different analyzer directions measured in free space.

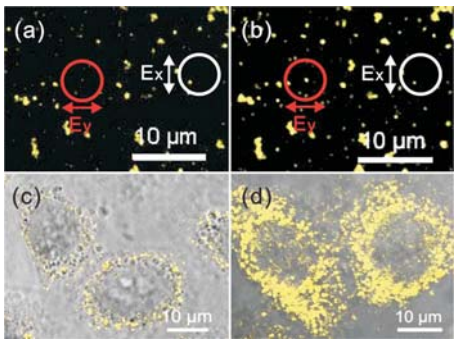

FIG. 3. (Color online) Two-photon photoluminescence imaging of gold nanorods on a coverglass [(a) and (b)] and labeled to cancer cells [(c) and (d)], respectively. (a) and (c) are for linear polarization. (b) and (d) are for radial polarization.

and is consistent with the prediction by the vectorial Debye diffraction theory used in this letter.[9] High quality GNRs that have an average length of 45 nm and an aspect ratio of 4 (Ref. 10) with a longitudinal absorption peak at wavelength 780 nm were prepared using the seeded synthetic method.[11]

There are several methods to produce radially polarized beams, including using space-variant dielectric subwavelength gratings, a conical Brewster prism and interferometers.[12–14] In our work a radially polarized beam with a high quality was produced by simply inserting a twisted nematic liquid crystal RPC into the beam path shown in Fig. 2(a). The RPC operates with a high conversion efficiency (70%–80%) in a broad wavelength region (400–1700 nm).[15] Figure 2(b) presents the characteristic hollow beam profile of a radially polarized beam in free space. Figures 2(c) and 2(d) show the polarization intensity distributions of the beam after passing a 45° and a 90° analyzer, respectively. The angular polarization uniformity with an approximately 5% difference of the intensity in the transverse plane in free space is illustrated in Fig. 2(e).

To examine the effectiveness of the laser beam profiles, TPF images of a given GNR sample on a coverglass were taken at the same incident power under linear and radial polarization illumination, as shown in Figs. 3(a) and 3(b), respectively. It is obvious that Fig. 3(b) presents a much enhanced fluorescence image because more GNRs are efficiently excited under radial polarization illumination owing to its three-dimensional polarization distribution in the focal volume, as suggested by the theoretical calculation in Figs. 1(e)–1(g). For example, as indicated by the red circle under linear polarization excitation [Fig. 3(a)], weak fluorescence is observed because the longitudinal axes of GNRs are aligned with E_y component in the focal volume whose strength is two orders of magnitude weaker than that of the E_x component [Figs. 1(a) and 1(c)]. However, strong fluorescence can be seen in the same region under radial polarization illumination [Fig. 3(b)] suggesting the GNRs are efficiently excited by the E_y component. Strong fluorescence under linear polarization excitation is only possible when the longitudinal axes of GNRs are aligned with the E_x direction [the white circle in Fig. 3(a)].

Human cervical cancer cells were used here for both imaging and therapy. The cultivation process of cells was detailed else where.[10,16] Figures 3(c) and 3(d) show the TPF imaging of GNR labeled living cancer cells in the same well subject to linearly and radially polarized beam illumination

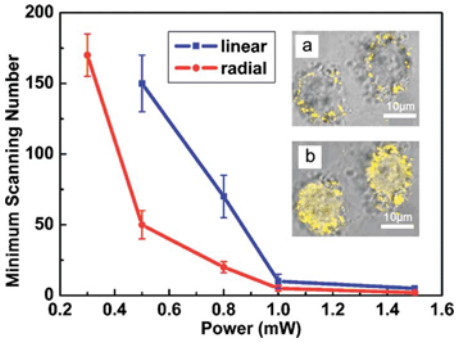

FIG. 4. (Color online) Minimum scanning number vs incident power for photothermal therapy of cancer cells labeled with gold nanorods under linear polarization and radial polarization illumination. Insets: two-photon photoluminescence images (a) before photothermal therapy and (b) after photothermal therapy.

under the same conditions, respectively. It can be seen that GNRs were well distributed on the membrane of the cancer cells. As expected, a fluorescence enhancement was observed when the randomly orientated GNRs attached to cancer cells were excited under radial polarization illumination [Fig. 3(d)].

Following the TPF imaging of cells labeled with GNRs, fresh medium (0.3 mL) and ethidium bromide (EB) (2 μg/mL) in PBS (0.6 mL) were added to each well. EB served as an indicator of cell viability as it can only penetrate into dead cells with a compromised membrane and stain their nucleus. An illumination wavelength at 740 nm, which is off the nanoparticle resonance, was employed to excite EB for imaging the membrane integrity and viability of cells. The incident laser power for the PTT was kept to be the same for the two polarization illumination conditions. Figure 4 presents the dependence of the minimum scanning number required to kill the cancer cells on the incident laser power at wavelength 780 nm under linear polarization and radial polarization illumination, respectively. The insets (a) and (b) of Fig. 4 are the images of the cancer cells labeled with GNRs under radial polarization illumination at 1.5 mW and the EB staining of the nucleus in the image of the same cells killed by the laser after the PTT, respectively. Cancer cells were clearly killed after 170 scans (one scan lasts for 1.05 s and the scanned area is 60 μm$\times$60 μm) at the incident power of 0.3 mW using the radially polarized beam while no cells were found dead after 500 scans at the same power when exposed to the linearly polarized beam. The laser energy for the PTT of cancer cells under radial polarization illumination can be significantly reduced from half to one fifth of that required for linearly polarized beam illumination for the incident power ranging from 1.5 to 0.5 mW. The energy threshold for PTT with a radially polarized beam is 9.3 mJ/cm^2, which is only 9.3% of the medical safety level.

In conclusion, it has been demonstrated that a radially polarized beam is an efficient laser mode to excite randomly oriented GNRs labeled to cancer cells owing to their three-dimensional polarization distribution in the focal volume. The experimental results for cancer cell PTT show the radially polarized beam can significantly reduce the energy fluence to one fifth of that required for a linearly polarized beam, which is more than one order of magnitude lower than the medical safety level.

This work was supported by the Australian Research Council (ARC).

[1]L. R. Hirsch, R. J. Stafford, J. A. Bankson, S. R. Sershen, B. Rivera, R. E. Price, J. D. Hazle, N. J. Halas, and J. L. West, Proc. Natl. Acad. Sci. U.S.A. **100**, 13549 (2003).
[2]S. E. Skrabalak, L. Au, X. Lu, X. Li, and Y. Xia, Nanomedicine **2**, 657 (2007).
[3]Z. Zhang, S. H. Lee, C. W. Gan, and S.-S. Feng, Pharm. Res. **25**, 1925 (2008).
[4]X. Huang, I. H. El-Sayed, W. Qian, and M. A. El-Sayed, J. Am. Chem. Soc. **128**, 2115 (2006).
[5]L. Tong, Y. Zhao, T. B. Huff, M. N. Hansen, A. Wei, and J.-X. Cheng, Adv. Mater. **19**, 3136 (2007).
[6]P. Zijlstra, J. W. M. Chon, and M. Gu, Nature (London) **459**, 410 (2009).
[7]American National Standards Institute, *American National Standard for Safe Use of Lasers ANSI Z136.1* (Laser Institute of America, Orlando, 2000).
[8]M. Gu, *Advanced optical imaging theory* (Springer, Heidelberg, 2000).
[9]B. Jia, X. Gan, and M. Gu, Opt. Express **13**, 6821 (2005).
[10]J. Li, D. Day, and M. Gu, Adv. Mater. **20**, 3866 (2008).
[11]T. K. Sau and C. J. Murphy, Langmuir **20**, 6414 (2004).
[12]Z. Bomzon, G. Biener, V. Kleiner, and E. Hasman, Opt. Lett. **27**, 285 (2002).
[13]Y. Kozawa and S. Sato, Opt. Lett. **30**, 3063 (2005).
[14]S. C. Tidwell, D. H. Ford, and W. D. Kimura, Appl. Opt. **29**, 2234 (1990).
[15]M. Stalder and M. Schadt, Opt. Lett. **21**, 1948 (1996).
[16]A. Gole and C. J. Murphy, Chem. Mater. **17**, 1325 (2005).